Two major sudden stratospheric warmings during winter 2023/2024

Simon H. Lee[1], **Amy H. Butler**[2] and **Gloria L. Manney**[3,4]

[1] *School of Earth and Environmental Sciences, University of St Andrews, St Andrews, UK*
[2] *NOAA Chemical Sciences Laboratory, Boulder, Colorado, USA*
[3] *NorthWest Research Associates, Inc, Socorro, New Mexico, USA*
[4] *Department of Physics, New Mexico Institute of Mining and Technology, Socorro, New Mexico, USA*

Introduction

Abrupt warmings of the wintertime high-latitude stratosphere 10–50km above the surface in the Northern Hemisphere were first observed over 70 years ago (Scherhag, 1952). Subsequently, these events have become known as 'sudden stratospheric warmings' (SSWs), in which the temperature of the stratosphere can rise by over 50°C in a few days (e.g. Baldwin *et al*., 2021; Lee, 2021). SSWs involve disruption to the westerly circulation of the stratospheric polar vortex by planetary waves (large wavelength Rossby waves), usually of zonal wavenumbers 1–3 (i.e. between one and three waves around a latitude circle). If the disruption is sufficiently strong, then – at least in the zonal mean – the westerlies are temporarily replaced by easterlies. These events are termed *major* SSWs to distinguish them from more frequent *minor* warmings[1] and are also distinct from springtime 'final warmings' in which the vortex does not recover due to the seasonal cycle in incoming solar radiation (e.g. Butler and Domeisen, 2021). On average, SSWs have been observed to occur approximately six times per decade in the Arctic (Butler *et al*., 2017), but there is marked decadal variability in their frequency (Dimdore-Miles *et al*., 2021). The spatial structure of the vortex during an SSW can take on a wide array of forms (Chen *et al*., 2024), but SSWs are most simply classified as either vortex *displacement* events (predominantly wavenumber 1, where the vortex is shifted away from the pole) or *split* events (predominantly wavenumber 2, in which the vortex splits into two or more smaller vortices) (e.g. Charlton and Polvani, 2007).

The wave activity that drives SSWs can be generated by tropospheric phenomena that constructively interfere with, and therefore amplify, the stationary waves generated by the mountains and land-sea temperature contrasts in the Northern Hemisphere mid-latitudes (e.g. Smith and Kushner, 2012). Examples of such tropospheric phenomena include blocking (e.g. Bao *et al*., 2017), extratropical cyclones (e.g. Cho *et al*., 2022) and tropical sources of poleward-propagating Rossby waves such as the Madden-Julian Oscillation (MJO; e.g. Garfinkel *et al*., 2012a) and the El Niño-Southern Oscillation (ENSO; e.g. Polvani *et al*., 2017). A key pathway for the latter is the modulation of the Aleutian Low (e.g. Garfinkel and Hartmann, 2008). Alternatively, the state of the stratosphere can preferentially focus waves towards the polar vortex and/or generate wave activity internally (Albers and Birner, 2014), meaning that wave activity propagating up from the troposphere need not be anomalous (de la Cámara *et al*., 2019). In addition, the quasi-biennial oscillation (QBO) in the equatorial stratosphere, which is characterised by a descending transition from easterly to westerly winds every ~28 months, can modulate the strength of the polar vortex, with a weaker vortex and more frequent SSWs when the QBO is easterly in early winter (Holton and Tan, 1980; Gray *et al*., 2018). This is usually attributed to preferential focusing of wave activity onto the vortex when the QBO is easterly (because Rossby waves cannot propagate into easterlies), but the full mechanism may be more complex (Garfinkel *et al*., 2012b).

In the past few decades, SSWs have gained particular attention because of their downward influence on tropospheric weather patterns (Baldwin and Dunkerton, 2001; Hitchcock and Simpson, 2014) and the associated implications for subseasonal-to-seasonal prediction (Domeisen *et al*., 2020). For up to around 2 months following SSWs, the Atlantic eddy-driven (polar) jet stream is on average shifted equatorward (Maycock *et al*., 2020), associated with the negative phase of the North Atlantic Oscillation (NAO)/Northern Annular Mode (NAM) and an increased likelihood of Greenland blocking (Beerli and Grams, 2019). These circulation anomalies drive concomitant temperature and precipitation anomalies; notably, mid-latitude cold-air outbreaks (particularly in Europe) are more likely when the polar vortex is weakened (Kolstad *et al*., 2010), which can lead to a detectable increase in mortality (Charlton-Perez *et al*., 2021). However, only around two-thirds of SSWs are followed by a persistently negative tropospheric NAM (Karpechko *et al*., 2017). Various explanations for this have been proposed, including differences in the stratospheric evolution (e.g. Kodera *et al*., 2016) and destructive interference by tropospheric forcing (e.g. Knight *et al*., 2021). In particular, the surface response to SSWs is strongly modulated by the extent to which the weak vortex anomaly reaches the lower stratosphere (White *et al*., 2020).

Following a period of four consecutive winters with no SSWs (2013/2014–2016/2017 inclusive), only two of the past seven winters have seen no SSWs (2019/2020 and 2021/2022). This 'active' period began with the February 2018 SSW, which was followed by the so-called 'Beast from the East' cold-air outbreak in northwest Europe (Greening and Hodgson, 2019) and sparked wider scientific, commercial and public interest in the events. During the winter of 2023/2024, two major SSWs occurred, which is a relatively rare event – although sensitive to the exact definition and dataset used, winters with two SSWs have occurred only around once per decade on average, and 2024 was the first winter to see two events since at least 2010. The two SSWs also evolved very differently, with different possible impacts on the tropospheric evolution. In this article, we summarise the evolution of the SSWs and discuss their wider climatic context and associated stratosphere–troposphere coupling.

Data and methods

We base our analyses on the fifth-generation reanalysis produced by the European Centre for Medium-Range Weather Forecasts, ERA5

[1] Hereinafter, we use the term 'SSW' for major events only.

(Hersbach *et al.*, 2020; Soci *et al.*, 2024). Although ERA5 data stretch back to 1940, we consider data beginning in the winter of 1957/1958 as this coincides with increased stratospheric observations as part of the International Geophysical Year. 10hPa zonal winds used to define the SSW dates are obtained on a 0.25° grid at 6-hourly temporal resolution; otherwise, data are obtained on a 1.5° grid once-daily at 0000 UTC since the large-scale fields are qualitatively insensitive to the coarser spatiotemporal resolution. We also compared the dates of the SSWs in winter 2023/2024 obtained from ERA5 with those computed from daily-mean JRA-3Q (Japanese Reanalysis for Three Quarters of a Century; Kosaka *et al.*, 2024) and MERRA-2 (Modern-Era Retrospective analysis for Research and Applications, version 2; Gelaro *et al.*, 2017) reanalysis data and obtained the same results.

SSW definition

To classify SSWs, we follow the well-established algorithm of Charlton and Polvani (2007). While some small adjustments have been proposed to the Charlton and Polvani (2007) algorithm (Butler and Gerber, 2018), they typically only influence late-March SSWs that are not well separated from the final warming. Hence, in this article, we follow Charlton and Polvani (2007) and define SSWs as a reversal of the daily-mean 10hPa 60°N westerly zonal-mean zonal winds (hereafter, U10-60) to easterlies between November and March. Once a reversal has occurred, the zonal winds must return to westerly for at least 20 consecutive days before another SSW can be defined (the results for 2024 are unchanged if the 30-day separation criterion of Butler and Gerber (2018) is used instead). The separation criterion is motivated by the typical radiative timescales in the mid-stratosphere during midwinter and ensures that the detected events are dynamically separable. Using this definition, we obtain 44 SSWs in the 67 winters from 1957/1958 through 2023/2024 (a rate of 6.6 SSWs per decade), with two SSWs occurring in the winters of 1965/1966, 1968/1969, 1970/1971, 1987/1988, 1998/1999, 2001/2002, 2009/2010 and 2023/2024.

Northern Annular Mode

The Northern Annular Mode (NAM), also known as the Arctic Oscillation, is the leading pattern of atmospheric variability in the Northern Hemisphere extratropics. In the troposphere, it is strongly correlated with the NAO (the extent to which the two are meaningfully different has been debated; e.g. Feldstein and Franzke, 2006). Various methods exist for defining the NAM (Baldwin and Thompson, 2009). Here, we use standardised anomalies of daily 60–90°N geopotential heights at each pressure level, where the daily mean and standard deviation are computed over 1 January 1958–31 December 2023 and smoothed with a 30-day running mean. Trends in geopotential height arising from global-mean temperature trends are accounted for by subtracting the global-mean at each day and pressure level (similar to Gerber and Martineau, 2018).

Eddy heat flux

To diagnose vertical wave propagation, we use the zonally averaged meridional eddy heat flux (i.e. the zonal mean of the product of the departures of the meridional wind and temperature from their respective zonal means, $[v^*T^*]$). This is proportional to the vertical component of the Eliassen–Palm wave activity flux, such that positive eddy heat flux indicates upward wave propagation and negative eddy heat flux indicates downward wave propagation. Upward propagating Rossby wave activity converges in the stratosphere and exerts a westward drag (i.e. an easterly acceleration) on the westerly zonal winds. Here, we average eddy heat flux across 45–75°N and show standardised anomalies with respect to a 30-day running calendar day mean and standard deviation computed over 1 January 1958–31 December 2023.

Climate background: ENSO and the QBO

ENSO and the QBO both modulate the strength of the Arctic stratospheric polar vortex and are predictable several months in advance, making them potentially useful for extended-range polar vortex prediction. During winter 2023/2024, moderate-to-strong El Niño conditions were present, with the three-monthly mean Oceanic Niño Index peaking at +2.0°C during November–January. The QBO was in the descending easterly phase; equatorial zonal winds were easterly at 50hPa by November–December, but relatively weak. This combination of a relatively weak easterly QBO and moderate/strong El Niño (Niño 3.4 > 1.5°C) is rare (Figure 1). Of the El Niño winters with an easterly QBO, El Niño events of similar strength occurred in 1965/1966, 1972/1973 and 1993/1994, but the easterly QBO was much stronger in 1966 and 1973, and only very weakly easterly in 1994. As a result, since 1957/1958, there are no clearly comparable winters to 2023/2024 in terms of the joint ENSO-QBO phase space.

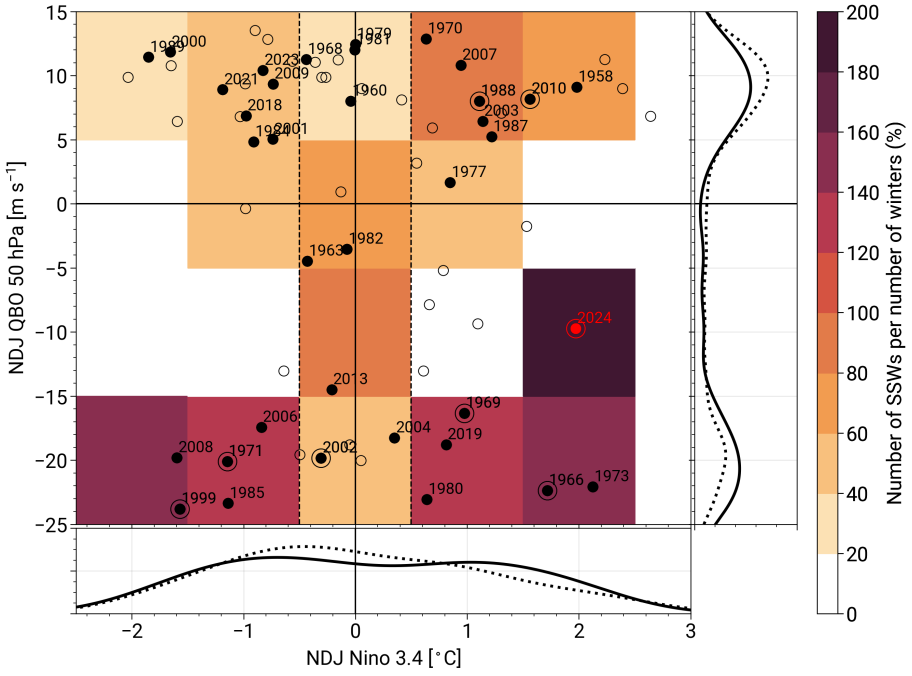

Figure 1. Scatter plot of historical November–January (NDJ) averaged ENSO (Niño 3.4 Oceanic Niño Index) and QBO winds at 50hPa, from 1958 to 2024 (circle markers). Filled circles indicate winters (November–March) that had one SSW; filled circles with an open circle around them are winters that had two SSWs. The 2023/2024 winter is marked by a red circle. Vertical dashed lines at ±0.5°C show thresholds for La Niña and El Niño winters. The heat map shading shows the number of observed SSWs per winter within the ENSO/QBO thresholds defined by each square. Below and to the right of the scatterplot/heat map, distributions of NDJ ENSO and QBO winters for all years (dotted line) and only winters with at least one SSW (solid line) are shown. These distributions are represented by a kernel-density estimate using Gaussian kernels. For the bimodal QBO distribution, the bandwidth has been adjusted to better resolve the actual distribution.

In the short observational record, SSWs have been more likely to occur during easterly QBO and either El Niño or La Niña (rather than neutral) conditions. However, some model experiments suggest that the combination of El Niño and easterly QBO is most favourable for SSWs (Walsh *et al*., 2022). Irrespective of the QBO, in the historical record SSWs have occurred with equal frequency during El Niño and La Niña, and more often than during ENSO neutral conditions. Therefore, while the precise risk from each ENSO-QBO combination still proves challenging to discern, the presence of an easterly QBO and an active El Niño phase suggested a broadly elevated risk of a weakened stratospheric polar vortex during winter 2024. The rarity of winters with two SSWs limits drawing any robust conclusions from observations about any potential ENSO-QBO modulation, but we note that two SSWs have not yet occurred during a La Niña winter with a westerly QBO.

Overview of the winter

We begin by examining the evolution of the stratospheric polar vortex during the winter, as shown by the time series of U10-60 in Figure 2(a). During December, zonal winds remained close to 30ms^{-1}, near or slightly below average. Subsequently, the vortex weakened rapidly in the opening week of January, with U10-60 reaching a minimum of 12ms^{-1} on 7 January. This marked the first minor warming of the winter. Over the next week, the vortex remained disturbed, and another rapid deceleration culminated in the reversal of the daily-mean U10-60 on 16 January and the occurrence of a major SSW. However, the deceleration ceased almost immediately; zonal winds remained only very weakly easterly for just 2 days, and the vortex rapidly re-intensified thereafter – almost as quickly as it had weakened.

In mid-February, another minor warming episode occurred, with a rapid deceleration of the zonal winds from 33ms^{-1} on 10 February to 0.4ms^{-1} on 19 February – remarkably close to becoming a major SSW. Despite this extremely fine margin, none of the three modern reanalysis datasets considered here (ERA5, MERRA-2 and JRA-3Q) show easterly daily-mean U10-60 on this date. A slow recovery of the zonal winds then followed, before another deceleration began at the start of March. The second major SSW of the winter then occurred on 4 March, as daily-mean U10-60 became easterly. This event was more intense than the January event; easterly winds persisted for 21 consecutive days, reaching a minimum of −20ms^{-1} on 15 March. By April, the seasonal increase in solar radiation in the Arctic meant the recovery of the vortex was minimal. The final warming then occurred on 29 April, over 2 weeks later than the historical median date of 12 April (Butler and Domeisen, 2021). However, a later-than-average final warming is common during winters with an SSW, largely due to the slow recovery of the vortex post-SSW preventing the occurrence of another warming.

When comparing with 42 previously observed SSWs, the evolution (Figure 3a) and strength (Figure 3b) of both events in winter 2024 were unusual. The re-intensification of the vortex following the 16 January SSW was exceptional in the historical record (per ERA5), setting records for westerly U10-60 5–9 days after an SSW. The easterlies following the SSW were the 4th weakest, and it was the weakest SSW by this metric to occur in January. In contrast, the easterlies following the 4 March SSW were the 7th strongest on record and the strongest on record for a March SSW by a wide margin. Furthermore, the unusual intensity of the minor warming on 19 February and its proximity to the 4 March event resulted in the weakest daily-mean westerly U10-60 on record during the 4 weeks prior to a major SSW. The two SSWs themselves occurred only 48 days apart, which is the second shortest period between SSWs after the 43 days between the events of 9 February and 24 March 2010, and similar to the 49 days between the 30 December 2001 and 17 February 2002 events.

Some reports issued during the winter[2] referred to the occurrence of three SSWs, but established criteria for defining SSWs classify only two major events. No winter in the observational record has seen three SSWs, but estimates from a large ensemble of the Met Office GloSea5 model give an approximate return period of 1-in-250 years (Ineson *et al*., 2024). Nonetheless, 6-hourly ERA5 data do show U10-60 becoming very briefly easterly at 0000 UTC (−1.6ms^{-1}) and

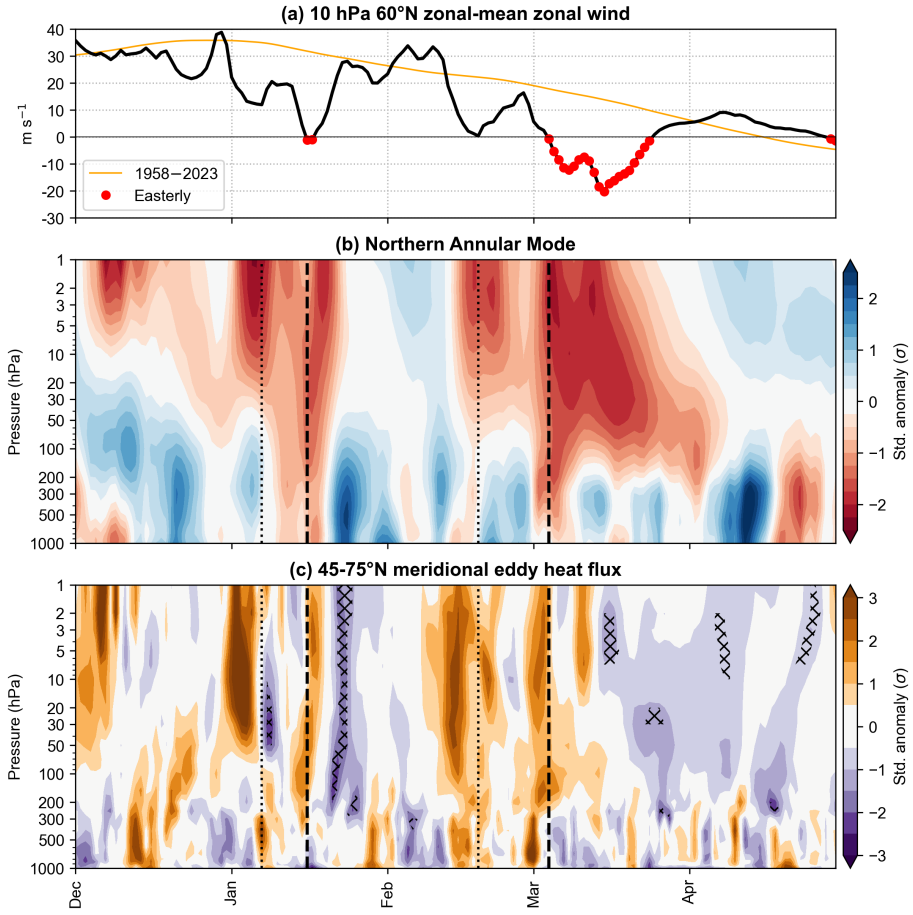

Figure 2. Evolution of the Arctic stratospheric polar vortex during winter 2023/2024 based on ERA5 reanalysis. (a) Daily-mean zonal-mean zonal winds at 10 hPa and 60°N. Red markers indicate days with daily-mean easterly winds. The orange line shows the 1958–2023 climatology, smoothed with a 30-day centred running mean. (b) Pressure–time cross-section of the Northern Annular Mode index (for methodological details, see main text). (c) Pressure–time cross-section of standardised anomalies of 45–75°N average meridional eddy heat flux. In (b) and (c), vertical black dashed lines denote the dates of the two major SSWs (16 January and 4 March 2024) and dotted black lines denote the dates of minima in U10-60 associated with two minor warmings (7 January and 19 February 2024). In (c), black cross-hatching denotes days where the total eddy heat flux (i.e. not the anomaly) was negative. Anomalies are expressed with respect to the 1958–2023 climatology.

[2] https://blog.metoffice.gov.uk/2024/03/06/one-in-250-year-event-underway-high-in-the-atmosphere/ [Accessed 30 October 2024].

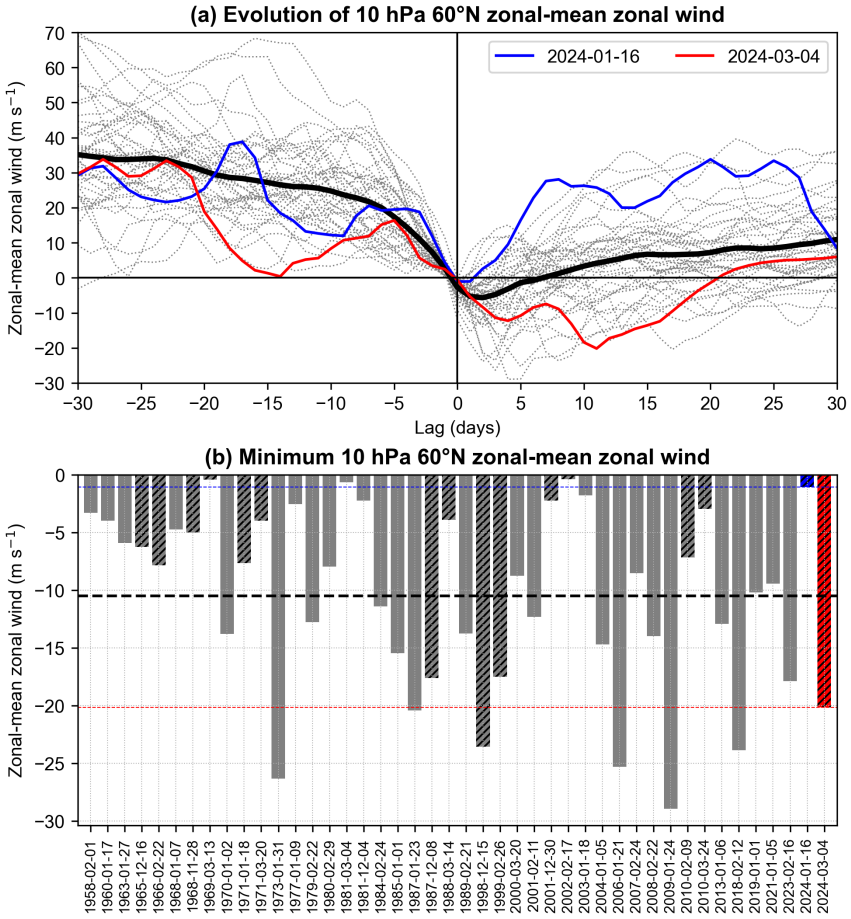

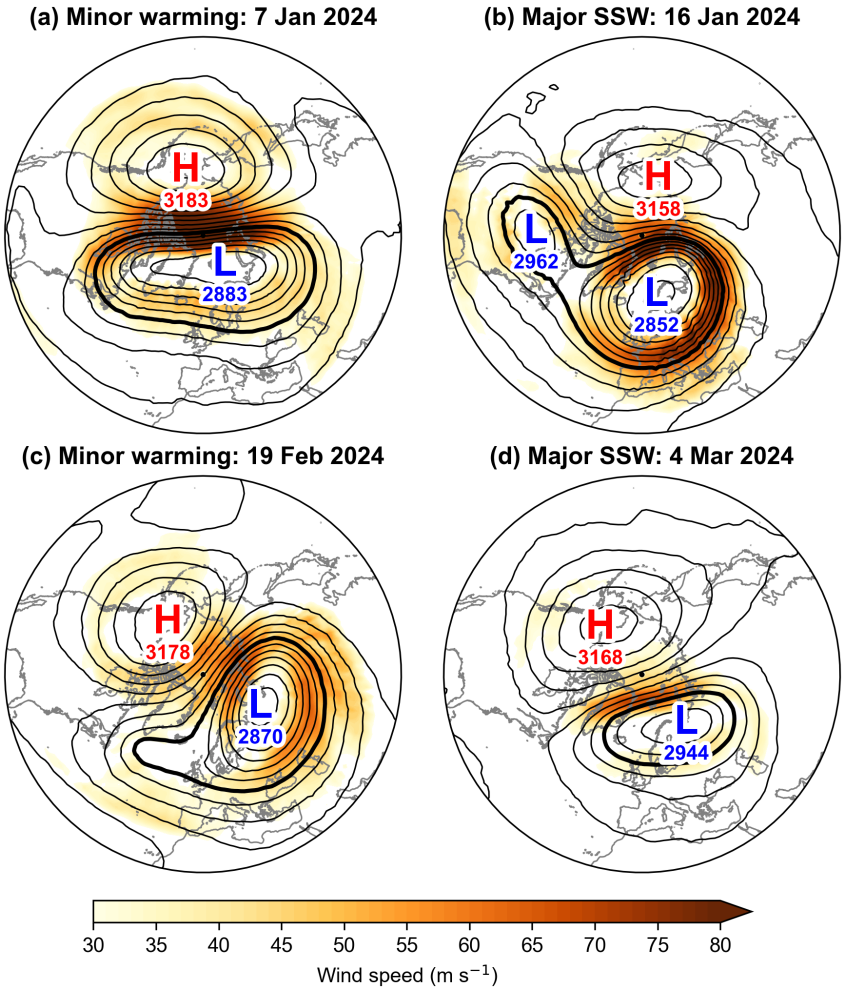

Figure 3. (a) Evolution of daily-mean U10-60 for 30 days before to 30 days after 42 SSWs in 1957/1958–2022/2023 (dotted grey lines), the 16 January 2024 SSW (blue line), and the 4 March 2024 SSW (red line). (b) Minimum U10-60 in the period 0–30 days after 44 SSWs in 1957/1958–2023/2024. The horizontal black dashed line denotes the average. Hatched bars denote instances of two SSWs in a single winter.

0600 UTC (−1.4ms^{-1}) on 19 February, sufficient to turn the 24-h centred running mean (as opposed to the calendar day mean) weakly negative at 0000 and 0600 UTC on the 19th (−0.5ms^{-1}). However, if one were to consider the brief, sub-daily reversal of U10-60 on 19 February as a 'major' event, then the reversal on 4 March would not be classified as a separate event because it occurred after only 13 consecutive days of westerly winds, rather than the widely used 20 (or even 30) days. These criteria are important to establish dynamically separable events, including relative to their tropospheric impacts. The evolution of the NAM (Figure 2b) also supports the interpretation of two, not three, major SSWs.

Dynamical evolution

Having summarised the key events in the Arctic stratosphere during winter 2023/2024, we now look more closely at the dynamics. The minor warming on 7 January was preceded by anomalous wave activity in only the stratosphere (mainly above 50hPa, where it exceeded 3 standard deviations); wave activity was either average or below average in the troposphere at that time (Figure 2c). This provides a clear example of stratospheric variability *not* directly related to anomalous tropospheric wave forcing (e.g. de la Cámara *et al.*, 2019). The 7 January minor warming was dominated by wavenumber 1, with an intensified stratospheric Aleutian High and a displaced, elongated vortex (Figure 4a). However, eddy heat flux then turned negative immediately afterwards between 50 and 10hPa, indicative of downward-propagating wave activity. The resultant divergence of wave activity in the mid-stratosphere and associated zonal wind acceleration likely played a key role in this event failing to become a major warming. Nonetheless, the vortex throughout

Figure 4. Maps showing 10hPa wind speeds (filled) and geopotential height (contours) from ERA5 reanalysis at 0000 UTC on (a) 7 January 2024, during a minor warming, (b) 16 January 2024, during a major SSW, (c) 19 February 2024, during a minor warming, and (d) 4 March 2024, during a major SSW. Contours every 20 decametres (dam), with the 3000 dam contour thickened.

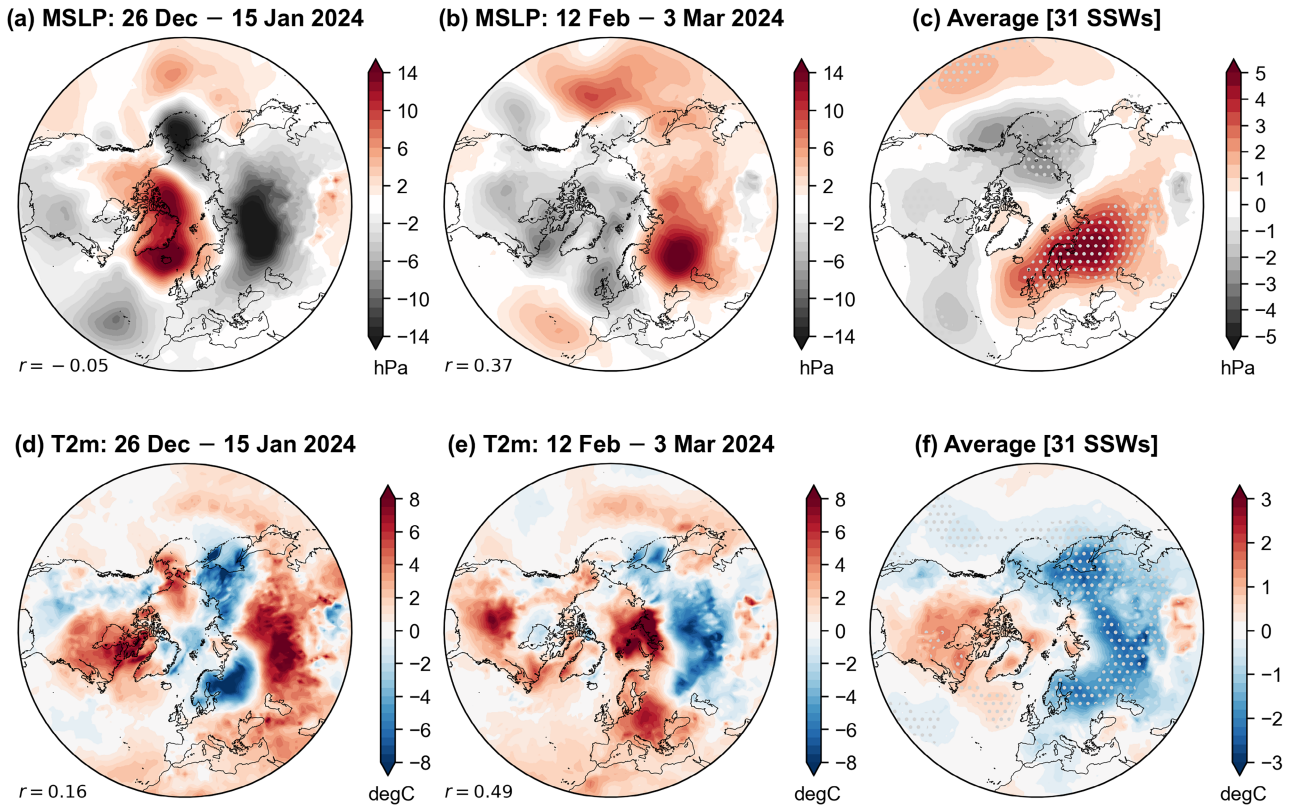

Figure 5. (a–c) Average MSLP anomalies (hPa) for the 21 days before (a) the 16 January 2024 SSW, (b) the 4 March 2024 SSW and (c) the average across 31 SSWs in 1979–2024. In (a) and (b), the area-weighted pattern correlation (r) with the composite map is also shown in the lower left. (d–f) As in (a–c) but for 2m temperature (°C). Anomalies are expressed with respect to the 1991–2020 climatology. In (c) and (f), stippling indicates the mean is significantly different from zero at the 5% level, according to a bootstrap resampling test with 10 000 iterations.

the column was weakened, with a negative NAM coupled between the stratosphere and troposphere (Figure 2b).

Subsequently, another burst of anomalous wave activity occurred – this time linked to anomalous upper-tropospheric wave activity – resulting in the 16 January major SSW. This event was also dominated by wavenumber 1, but the vortex showed some signs of splitting (wavenumber 2) with the main vortex displaced above Scandinavia and a smaller lobe of the vortex over northern Canada (Figure 4b). Splitting of the vortex was more substantial in the lower stratosphere; this appeared to be due to the upward influence of a blocking anticyclone over Greenland (Figure 5a; itself perhaps linked to the effect of the earlier minor warming).[3] What followed was an extremely unusual evolution for a major SSW. Eddy heat flux became negative throughout the stratosphere, indicating large-scale downward wave propagation; the divergence of wave activity led to an abrupt restrengthening of the vortex and a termination of the negative NAM. In the troposphere, a very strongly positive NAM developed – opposite to the average evolution after a major SSW, but in agreement with the behaviour of 'reflecting' SSWs (Kodera *et al.*, 2016). Hence, the NAM in both the stratosphere and troposphere *prior* to the major SSW more closely resembled the average evolution *after* a major SSW than what followed. Consistent with the absence of anomalous tropospheric wave activity, the MSLP and 2m temperature anomalies prior to the SSW (Figure 5a,d) do not strongly resemble average SSW precursor patterns (Figure 5c,f), except for the deepened Aleutian Low.

By early February, the vortex in the mid-upper stratosphere had become stronger-than-average (positive NAM) and coupled to the positive NAM in the troposphere (Figure 2b). At this time, wave activity increased in both the stratosphere and troposphere, leading to the abrupt weakening of the vortex and the onset of a negative NAM in the stratosphere, but it was insufficient to induce a major SSW. The onset of this warming immediately after the development of a positive NAM throughout the column suggests that the strengthened vortex served as a coherent vertical wave guide. Once again, this event was dominated by wavenumber 1, although relative to the earlier disruptions, it was rotated slightly anticlockwise, with the main vortex displaced over northern Siberia (Figure 4c). Then, at the start of March, a burst of anomalous wave activity in the troposphere moved up into the stratosphere, ultimately leading to the second major SSW of the winter. The anomalous tropospheric wave activity is consistent with the presence of an anomalous anticyclone over the Ural Mountains ('Ural blocking') prior to the SSW (Figure 5b), which is a common tropospheric precursor of SSWs (Figure 5c) (Kolstad and Charlton-Perez, 2011). Spatially, the 4 March event was similar to the 19 February minor warming, but the integrated effect of the wave activity over the previous weeks meant the vortex had been progressively eroded and warmed; the geopotential height in the core of the 10hPa vortex on 4 March was 74 dam higher, and the vortex itself was much smaller (Figure 4d). The evolution of the NAM in the stratosphere following the 4 March SSW more closely resembled the average evolution during an SSW; the negative NAM reached the lower stratosphere and persisted for around a month (Figure 2b). Wave activity in the stratosphere diminished after the SSW, owing to the strong and persistent easterlies (which do not support upward Rossby wave propagation) and disruption to the potential vorticity gradient that served as a wave guide around the edge of the vortex.

[3] See also https://www.climate.gov/news-features/blogs/polar-vortex/polar-vortex-acting [Accessed 19 August 2024].

Surface impacts

The 16 January SSW did not lead to the onset of a persistently negative NAM in the stratosphere (cf. Figure 2b), and the 'reflective' properties of the SSW were associated with the onset of a strongly positive NAM in the troposphere. Hence, average mean sea-level pressure (MSLP) and 2m temperature anomalies following the event (Figure 6a,d) did not resemble those associated with the average negative NAO response to an SSW (Figure 6c,f). This is unsurprising due to the lack of a negative stratospheric NAM and differs from situations in which there is a negative NAM in the stratosphere but minimal coupling with the troposphere (such as that seen following the SSW on 2 January 2019; Butler *et al*., 2020). Averaged over the 30 days after the event, North America was extremely warm (temperatures were more than 8°C above the 1991–2020 average across Canada) owing to an extended Pacific jet stream consistent with the presence of a strong El Niño (e.g. Shapiro *et al*., 2001). Europe was also generally warmer than average, with anomalously cyclonic conditions stretching from the Azores to Scandinavia leading to anomalous southwesterly flow across the continent and hence warmer-than-average conditions. Below normal temperatures were present across parts of Fennoscandia; this was a continuation of a persistent cold 'blob' that developed in late 2023 (Rantanen *et al*., 2024) and was stronger prior to the SSW (Figure 5d) than afterwards. Thus, it was unlikely related to the impact of the SSW.

During 21–24 January, storms *Isha* (named by the Met Office) and *Jocelyn* (named by Met Éireann) brought damaging winds to Britain, Ireland, and parts of northern Europe (Kendon, 2024). These storms developed from an intensified jet stream owing to a transient cold air outbreak in eastern North America downstream of an amplified Alaskan ridge. This large-scale pattern is often associated with wind extremes in northwest Europe (Riboldi *et al*., 2023) and is also similar to the response to reflecting SSWs in Kodera *et al*. (2016) and a positive NAO more generally.

In contrast, following the 4 March SSW, anomalously high pressure developed across Greenland and the Norwegian Sea, with anomalously low pressure to its south (Figure 6b) – a pattern more similar to the negative NAO/negative NAM-type response typically seen following major SSWs (Figure 6c). However, the anomalously low pressure centred west of Ireland once again led to anomalously southerly flow, resulting in above-average temperatures for Europe (Figure 6e). These circulation anomalies resemble the Atlantic Trough regime (Grams *et al*., 2017), which is associated with mild and unsettled conditions across northwest Europe and is common following SSWs (Beerli and Grams, 2019; Domeisen *et al*., 2020), despite its very different temperature footprint from that of the typical Greenland Blocking (negative NAO/NAM) response. Furthermore, the occurrence of this SSW in early spring (rather than mid-winter) may have influenced the surface response, because the structure of variability in the Atlantic (including the NAO) contracts poleward with the seasonal cycle.

Impacts on stratospheric chemistry

Polar stratospheric clouds (PSCs), also known as nacreous clouds, were widely observed across Europe in late December 2023 (e.g. Figure 7; Keates and Harris, 2024). These developed as the stratospheric Aleutian High strengthened, displacing the cold stratospheric vortex toward Europe (the slightly negative NAM in Figure 2(b) indicates a weak stratospheric disturbance). As seen in Figure 8(a), high-latitude (and thus vortex) minimum temperatures were unusually low in late November through late December 2023, with behaviour somewhat similar to that in late 2012. These unusually low temperatures, including several days on which ice PSCs were expected, accompanied by the vortex shifting away from the pole, are consistent with the widespread PSC observations.

Chemical reactions on the surfaces of PSCs convert chlorine from its reservoir forms into 'active' forms that can destroy ozone; chlorine monoxide (ClO) is the primary form of active

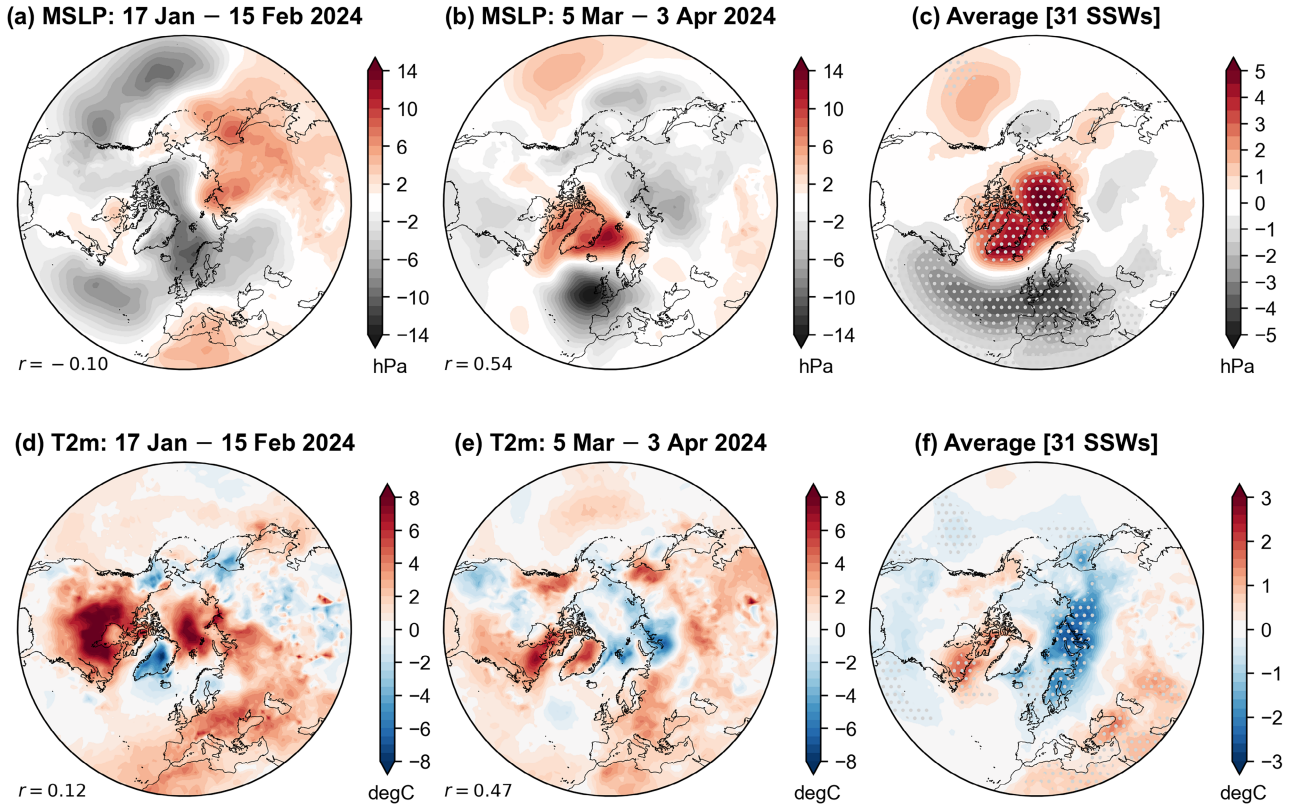

Figure 6. (a–c) Average MSLP anomalies (hPa) for the 30 days following (a) the 16 January 2024 SSW, (b) the 4 March 2024 SSW and (c) the average across 31 SSWs in 1979–2024. In (a) and (b), the area-weighted pattern correlation (r) with the composite map is also shown in the lower left. (d–f) As in (a–c) but for 2m temperature (°C). Anomalies are expressed with respect to the 1991–2020 climatology. In (c) and (f), stippling indicates the mean is significantly different from zero at the 5% level, according to a bootstrap resampling test with 10 000 iterations.

chlorine during sunlit periods (Solomon, 1999, and references therein). Figure 8(b) shows that the unusual cold in late December led to record-high vortex-averaged ClO values for those dates, rivalled only by those in late 2012. 2012/2013 and 2023/2024 are the only winters since 1991/1992 (when an earlier MLS instrument began measuring stratospheric composition) in which the temperatures and vortex evolution were conducive to such extremes. In both winters, the exceptionally high early winter ClO values arose from the combination of extensive chlorine activation in an unusually cold early winter vortex accompanied by the vortex moving away from the pole into regions that receive sunlight in midwinter (Manney *et al.*, 2015). In early January 2024, the vortex moved back towards the pole prior to the brief mid-January SSW, which temporarily increased temperatures above the PSC threshold and thus allowed chlorine deactivation to begin. After the prolonged SSW in January 2013, chlorine was gradually deactivated through the remainder of the winter; in 2024, however, temperatures soon dropped below PSC thresholds again until the February minor warming. Consistent with this, there was some additional chlorine activation during February 2024, though ClO values remained well below average.

Most chlorine-catalysed ozone depletion occurs in spring when the full stratospheric polar vortex receives sunlight (Solomon, 1999, and references therein), with ozone values in the lower stratospheric vortex typically increasing until about mid-January via descent of higher

Figure 7. Polar stratospheric clouds near Harrogate (North Yorkshire, UK; 54.0°N 1.5°W, looking south-east) illuminated by moonlight at 2217 UTC on 24 December 2023 (photograph by the lead author.)

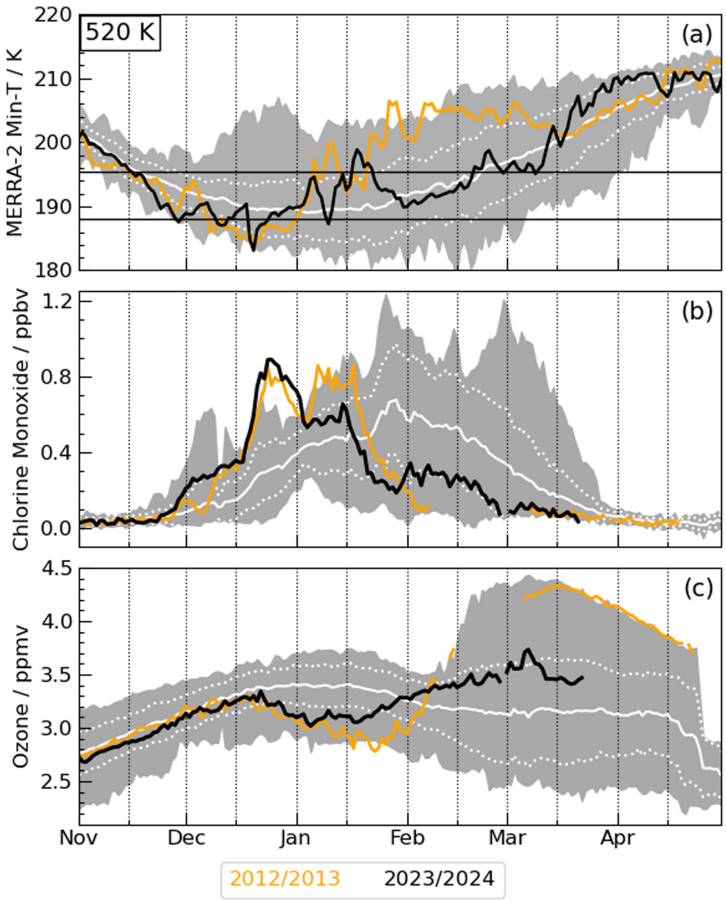

Figure 8. Timeseries on the 520K isentropic surface (near 21km altitude, 50hPa pressure) of (a) minimum highlatitude (poleward of 40°N) temperatures from the MERRA-2 reanalysis, and vortex averages of (b) Aura Microwave Limb Sounder (MLS) chlorine monoxide mixing ratios, and (c) MLS ozone mixing ratios (from v5 MLS data, Santee et al., *2021; Schwartz* et al., *2021). Black line shows the 2023/2024 winter, orange line the 2012/2013 winter (the only previous winter during the Aura mission with similar dynamical and composition evolution in December and January to that in 2023/2024); grey envelope shows the range over the Aura mission (2004/2005 through present, excluding 2012/2013 and 2023/2024, with mean and 1 standard deviation envelope shown as solid and dotted white lines, respectively. Black horizontal lines show the typical threshold below which polar stratospheric clouds (PSCs) can form, the upper line (higher threshold) for nitric acid trihydrate and the lower line for clouds primarily containing ice. PSC thresholds and vortex averages are calculated as described in Lawrence* et al. *(2018). Gaps in orange and black lines in (b) and (c) indicate times when the vortex was not defined by the metric used here (when it completely broke down from early February to early March 2013 and its final spring breakdown in late March in 2024 and late April in 2013).*

ozone. However, in late December 2023 and early January 2024, ozone values decreased substantially, similar to the anomalous behaviour in late 2012/early 2013. As reported by Manney *et al.* (2015) for 2012/2013, chemical ozone destruction was enabled by the exceptional chlorine activation coupled with vortices shifted to latitudes that received full sunlight during midwinter. Because the 2023/2024 vortex soon moved back over the pole (but with lower values of ClO), ozone began to increase as its changes were again dominated by descent of higher ozone in the vortex.

Arctic total column ozone is controlled primarily by dynamics even in the few exceptionally cold springs when chemical loss is a substantial factor (Manney *et al.*, 2011, and references therein); in spring 2024, the early vortex breakup, unusually high lower stratospheric temperatures, and lack of springtime chemical ozone loss all contributed to extremely high column ozone values (Newman *et al.*, 2024).

Conclusions

The two very different SSWs during early 2024 and their unusual evolution relative to previous events highlight the diversity of the phenomenon, which is still being revealed as the observational record lengthens. This further motivates studies involving large model ensembles, which can provide insight into rare events (e.g. Kolstad *et al.*, 2022; Ineson *et al.*, 2024). The rapid restrengthening of the vortex and dissipation of the negative NAM within a few days of the 16 January SSW meant that it quickly became evident that the SSW would not exert the canonical response in the troposphere. While the March SSW was more typical, observational evidence suggests that tropospheric impacts were still relatively muted. However, attributing impacts of SSWs solely from observations is difficult at best, and modelling studies would be required (similar to those used in the SNAPSI project; Hitchcock *et al.*, 2022).

The impact of the 2024 SSWs on polar chemical processing in the lower stratosphere shows (similar to that in 2013) the complex and nonlinear relationship of SSWs to that chemical processing, such that increasing temperatures above those at which such processing can occur may, because of changes in vortex morphology and position, have a short-term effect of temporarily increasing chemical ozone loss before chlorine deactivation can occur. Further studies should examine the relationship of the 2024 SSWs to polar processing in more detail, including exploring any impacts of the higher background water vapour levels from the 2022 Hunga volcanic eruption.

A clear avenue for future work is to examine the predictability of the two major SSWs in early 2024 on medium-range, subseasonal, and seasonal timescales. Notably, winter 2023/2024 was the first in which ECMWF produced 101-member, daily extended-range ensemble forecasts as part of the cycle 48r1 upgrade to the Integrated Forecasting System (Lang *et al.*, 2023). This will provide a new level of insight into the predictability of SSWs and their associated dynamics.

Acknowledgements

We thank two anonymous reviewers and the Editor RM for their helpful comments on our manuscript.

Author contributions

Simon H. Lee: Conceptualization; writing – original draft; writing – review and editing; visualization; formal analysis; methodology. **Amy H. Butler:** Writing – review and editing; writing – original draft; visualization; formal analysis. **Gloria L. Manney:** Writing – original draft; writing – review and editing; formal analysis; visualization.

Conflict of interest

S. H. Lee is Co-Editor-in-Chief of *Weather* but was not privy to the peer review process.

Funding information

G. L. Manney was supported by the Jet Propulsion Laboratory (JPL) Microwave Limb Sounder team under JPL subcontract #521127 to NWRA.

Data availability statement

ERA5 reanalysis data used in this study are freely available from the Copernicus Climate Data Store (https://doi.org/10.24381/cds.bd0915c6 for pressure-level data and https://doi.org/10.24381/cds.adbb2d47 for single-level data). MERRA-2 data are publicly available (Global Modeling and Assimilation Office (GMAO), 2015) at https://disc.sci.gsfc.nasa.gov/uui/datasets?keywords=%22MERRA-2%22 and Aura MLS Level-3 data for ozone (Schwartz *et al.*, 2021) and chlorine monoxide (Santee *et al.*, 2021) at https://disc.gsfc.nasa.gov/datasets?page=1&keywords=AURA%20MLS. The Oceanic Niño Index is publicly available at https://origin.cpc.ncep.noaa.gov/products/analysis_monitoring/ensostuff/ONI_v5.php. QBO data for 1958–2021 come from Freie Universität Berlin at https://www.geo.fu-berlin.de/met/ag/strat/produkte/qbo/qbo.dat; after 2021, data are obtained from NASA/Goddard at https://acd-ext.gsfc.nasa.gov/Data_services/met/qbo/QBO_Singapore_Uvals_GSFC.txt.

References

Albers JR, **Birner T**. 2014. Vortex preconditioning due to planetary and gravity waves prior to sudden stratospheric warmings. *J. Atmos. Sci.* **71**: 4028–4054.

Baldwin MP, **Ayarzagüena B**, **Birner T** ***et al***. 2021. Sudden stratospheric warmings. *Rev. Geophys.* **59**: e2020RG000708.

Baldwin MP, **Dunkerton TJ**. 2001. Stratospheric harbingers of anomalous weather regimes. *Science* **294**: 581–584.

Baldwin MP, **Thompson DW**. 2009. A critical comparison of stratosphere–troposphere coupling indices. *Q. J. R. Meteorol. Soc.* **135**: 1661–1672.

Bao M, **Tan X**, **Hartmann DL** ***et al***. 2017. Classifying the tropospheric precursor patterns of sudden stratospheric warmings. *Geophys. Res. Lett.* **44**: 8011–8016.

Beerli R, **Grams CM**. 2019. Stratospheric modulation of the large-scale circulation in the Atlantic–European region and its implications for surface weather events. *Q. J. R. Meteorol. Soc.* **145**: 3732–3750.

Butler AH, **Domeisen DI**. 2021. The wave geometry of final stratospheric warming events. *Weather Clim. Dyn.* **2**: 453–474.

Butler AH, **Gerber EP**. 2018. Optimizing the definition of a sudden stratospheric warming. *J. Clim.* **31**: 2337–2344.

Butler AH, **Lawrence ZD**, **Lee SH** ***et al***. 2020. Differences between the 2018 and 2019 stratospheric polar vortex split events. *Q. J. R. Meteorol. Soc.* **146**: 3503–3521.

Butler AH, **Sjoberg JP**, **Seidel DJ** ***et al***. 2017. A sudden stratospheric warming compendium. *Earth Syst. Sci. Data* **9**: 63–76.

Charlton AJ, **Polvani LM**. 2007. A new look at stratospheric sudden warmings. Part I: climatology and modeling benchmarks. *J. Clim.* **20**: 449–469.

Charlton-Perez AJ, **Huang WTK**, **Lee SH**. 2021. Impact of sudden stratospheric warmings on United Kingdom mortality. *Atmos. Sci. Lett.* **22**: e1013.

Chen Y-C, **Liang Y-C**, **Wu C-M** ***et al***. 2024. Exploiting a variational auto-encoder to represent the evolution of sudden stratospheric warmings. *Environ. Res.* **3**: 025006.

Cho H-O, **Kang M-J**, **Son S-W** ***et al***. 2022. A critical role of the North Pacific bomb cyclones in the onset of the 2021 sudden stratospheric warming. *Geophys. Res. Lett.* **49**: e2022GL099245.

de la Cámara A, **Birner T**, **Albers JR**. 2019. Are sudden stratospheric warmings preceded by anomalous tropospheric wave activity? *J. Clim.* **32**: 7173–7189.

Dimdore-Miles O, **Gray L**, **Osprey S**. 2021. Origins of multi-decadal variability in sudden stratospheric warmings. *Weather Clim. Dyn.* **2**: 205–231.

Domeisen DI, **Butler AH**, **Charlton-Perez AJ** ***et al***. 2020. The role of the stratosphere in subseasonal to seasonal prediction: 2. Predictability arising from stratosphere-troposphere coupling. *J. Geophys. Res.* **125**: e2019JD030923.

Domeisen DI, **Grams CM**, **Papritz L**. 2020. The role of north Atlantic–European weather regimes in the surface impact of sudden stratospheric warming events. *Weather Clim. Dyn.* **1**: 373–388.

Feldstein SB, **Franzke C**. 2006. Are the North Atlantic Oscillation and the north-

ern annular mode distinguishable? *J. Atmos. Sci.* **63**: 2915–2930.

Garfinkel C, **Hartmann D**. 2008. Different ENSO teleconnections and their effects on the stratospheric polar vortex. *J. Geophys. Res.* **113**: D18114.

Garfinkel CI, **Feldstein SB**, **Waugh DW *et al***. 2012a. Observed connection between stratospheric sudden warmings and the Madden-Julian oscillation. *Geophys. Res. Lett.* **39**: L18807.

Garfinkel CI, **Shaw TA**, **Hartmann DL *et al***. 2012b. Does the Holton–Tan mechanism explain how the quasi-biennial oscillation modulates the Arctic polar vortex? *J. Atmos. Sci.* **69**: 1713–1733.

Gelaro R, **McCarty W**, **Suárez MJ *et al***. 2017. The modern-era retrospective analysis for research and applications, version 2 (MERRA-2). *J. Clim.* **30**: 5419–5454.

Gerber EP, **Martineau P**. 2018. Quantifying the variability of the annular modes: reanalysis uncertainty vs. sampling uncertainty. *Atmos. Chem. Phys.* **18**: 17099–17117.

Global Modeling and Assimilation Office (GMAO). 2015. MERRA-2 inst3_3d_asm_nv: 3d, 3-Hourly, Instantaneous, Model-Level, Assimilation, Assimilated Meteorological Fields v5.12.4. Goddard Earth Sciences Data and Information Services Center (GES DISC): Greenbelt, MD, USA. [Accessed 10 August 2024].

Grams CM, **Beerli R**, **Pfenninger S *et al***. 2017. Balancing Europe's wind-power output through spatial deployment informed by weather regimes. *Nat. Clim. Chang.* **7**: 557–562.

Gray LJ, **Anstey JA**, **Kawatani Y *et al***. 2018. Surface impacts of the quasi biennial oscillation. *Atmos. Chem. Phys.* **18**: 8227–8247.

Greening K, **Hodgson A**. 2019. Atmospheric analysis of the cold late February and early March 2018 over the UK. *Weather* **74**: 79–85.

Hersbach H, **Bell B**, **Berrisford P *et al***. 2020. The ERA5 global reanalysis. *Q. J. R. Meteorol. Soc.* **146**: 1999–2049.

Hitchcock P, **Butler A**, **Charlton-Perez A *et al***. 2022. Stratospheric Nudging and Predictable Surface Impacts (SNAPSI): a protocol for investigating the role of stratospheric polar vortex disturbances in subseasonal to seasonal forecasts. *Geosci. Model Dev.* **15**: 5073–5092.

Hitchcock P, **Simpson IR**. 2014. The downward influence of stratospheric sudden warmings. *J. Atmos. Sci.* **71**: 3856–3876.

Holton JR, **Tan H-C**. 1980. The influence of the equatorial quasi-biennial oscillation on the global circulation at 50 MB. *J. Atmos. Sci.* **37**: 2200–2208.

Ineson S, **Dunstone NJ**, **Scaife AA *et al***. 2024. Statistics of sudden stratospheric warmings using a large model ensemble. *Atmos. Sci. Lett.* **25**: e1202.

Karpechko AY, **Hitchcock P**, **Peters DH *et al***. 2017. Predictability of downward propagation of major sudden stratospheric warmings. *Q. J. R. Meteorol. Soc.* **143**: 1459–1470.

Keates S, **Harris D**. 2024. Weather news. *Weather* **79**: 38–39.

Kendon M. 2024. Storms Isha and Jocelyn, 21 to 24 January 2024. https://www.metoffice.gov.uk/binaries/content/assets/metofficegovuk/pdf/weather/learn-about/uk-past-events/interesting/2024/2024_02_storms_isha_jocelyn.pdf

Knight J, **Scaife A**, **Bett PE *et al***. 2021. Predictability of European winters 2017/2018 and 2018/2019: contrasting influences from the tropics and stratosphere. *Atmos. Sci. Lett.* **22**: e1009.

Kodera K, **Mukougawa H**, **Maury P *et al***. 2016. Absorbing and reflecting sudden stratospheric warming events and their relationship with tropospheric circulation. *J. Geophys. Res.* **121**: 80–94.

Kolstad EW, **Breiteig T**, **Scaife AA**. 2010. The association between stratospheric weak polar vortex events and cold air outbreaks in the northern hemisphere. *Q. J. R. Meteorol. Soc.* **136**: 886–893.

Kolstad EW, **Charlton-Perez AJ**. 2011. Observed and simulated precursors of stratospheric polar vortex anomalies in the Northern Hemisphere. *Clim. Dyn.* **37**: 1443–1456.

Kolstad EW, **Lee SH**, **Butler AH *et al***. 2022. Diverse surface signatures of stratospheric polar vortex anomalies. *J. Geophys. Res.* **127**: e2022JD037422.

Kosaka Y, **Kobayashi S**, **Harada Y *et al***. 2024. The jra-3q reanalysis. *J. Meteorol. Soc. Jpn. Ser. II.* **102**: 49–109.

Lang S, **Rodwell M**, **Schepers D**. 2023. IFS upgrade brings many improvements and unifies medium-range resolutions. *ECMWF Newsletter* **176**: 21–28. https://www.ecmwf.int/en/newsletter/176/earth-system-science/ifs-upgrade-brings-many-improvements-and-unifies-medium

Lawrence ZD, **Manney GL**, **Wargan K**. 2018. Reanalysis intercomparisons of stratospheric polar processing diagnostics. *Atmos. Chem. Phys.* **18**: 13547–13579.

Lee SH. 2021. The stratospheric polar vortex and sudden stratospheric warmings. *Weather* **76**: 12–13.

Manney G, **Lawrence Z**, **Santee M *et al***. 2015. Polar processing in a split vortex: arctic ozone loss in early winter 2012/2013. *Atmos. Chem. Phys.* **15**: 5381–5403.

Manney GL, **Santee ML**, **Rex M *et al***. 2011. Unprecedented arctic ozone loss in 2011. *Nature* **478**: 469–475. https://doi.org/10.1038/nature10556

Maycock AC, **Masukwedza GI**, **Hitchcock P *et al***. 2020. A regime perspective on the north Atlantic Eddy-driven jet response to sudden stratospheric warmings. *J. Clim.* **33**: 3901–3917.

Newman PA, **Lait LR**, **Kramarova NA *et al***. 2024. Record high March 2024 Arctic total column ozone. *Geophys. Res. Lett.* **51**: e2024GL110924.

Polvani LM, **Sun L**, **Butler AH *et al***. 2017. Distinguishing stratospheric sudden warmings from ENSO as key drivers of wintertime climate variability over the North Atlantic and Eurasia. *J. Clim.* **30**: 1959–1969.

Rantanen M, **Hyvärinen O**, **Vajda A *et al***. 2024. The atmospheric 'cold blob' over Fennoscandia from October 2023 to January 2024. *Weather*. https://doi.org/10.1002/wea.4570

Riboldi J, **Leeding R**, **Segalini A *et al***. 2023. Multiple large-scale dynamical pathways for Pan–Atlantic compound cold and windy extremes. *Geophys. Res. Lett.* **50**: e2022GL102528.

Santee ML, **Livesey N**, **Read W *et al***. 2021. MLS/Aura Level 3 Daily Binned Chlorine Monoxide (ClO) Mixing Ratio on Zonal and Similar Grids V005. Goddard Earth Sciences Data and Information Services Center (GES DISC): Greenbelt, MD, USA. https://disc.gsfc.nasa.gov/datasets/ML3DZClO_005/summary?keywords=mls [Accessed 10 August 2024].

Scherhag R. 1952. Die explosionsartige stratosphaerenerwarmung des spaetwinters 1951/1952. *Ber. Deut. Wetterdienstes* **6**: 51.

Schwartz M, **Froidevaux L**, **Livesey N *et al***. 2021. MLS/Aura Level 3 Daily Binned Ozone (O3) Mixing Ratio on Zonal and Similar Grids V005. Goddard Earth Sciences Data and Information Services Center (GES DISC): Greenbelt, MD, USA. https://disc.gsfc.nasa.gov/datasets/ML3DZO3_005/summary?keywords=mls [Accessed 10 August 2024].

Shapiro M, **Wernli H**, **Bond N *et al***. 2001. The influence of the 1997–99 El Niño Southern Oscillation on extratropical baroclinic life cycles over the eastern North Pacific. *Q. J. R. Meteorol. Soc.* **127**: 331–342.

Smith KL, **Kushner PJ**. 2012. Linear interference and the initiation of extratropical stratosphere-troposphere interactions. *J. Geophys. Res.* **117**: D13107.

Soci C, **Hersbach H**, **Simmons A *et al***. 2024. The ERA5 global reanalysis from 1940 to 2022. *Q. J. R. Meteorol. Soc.* **150**: 4014–4048.

Solomon S. 1999. Stratospheric ozone depletion: a review of concepts and history. *Rev. Geophys.* **37**: 275–316.

Walsh A, **Screen J**, **Scaife A *et al***. 2022. Non-linear response of the extratropics to tropical climate variability. *Geophys. Res. Lett.* **49**: e2022GL100416.

White IP, **Garfinkel CI**, **Gerber EP *et al***. 2020. The generic nature of the tropospheric response to sudden stratospheric warmings. *J. Clim.* **33**: 5589–5610.

Correspondence to: S. H. Lee
shl21@st-andrews.ac.uk

doi: 10.1002/wea.7656